JOURNAL OF MATERIALS SCIENCE 19 (1984) 233–244

Nucleation kinetics in a glass–ceramic enamel

I. PENKOV, I. GUTZOW
Institute of Physical Chemistry, Bulgarian Academy of Sciences, 1040 Sofia, Bulgaria

The kinetics of nucleation in a glass-forming melt having the composition (in mol %) 71.80 SiO_2, 1.63 Al_2O_3, 23.20 Li_2O, 2.20 K_2O and 1.17 MoO_3 is investigated. X-ray analysis, DTA, optical and electron microscopy are used together with precise viscometric data to follow the crystallization process and to characterize the properties of both the initial melt and the resulting crystalline phase – the rhombic $Li_2O \cdot 2SiO_2$. By virtue of its composition, structure and properties the resulting semi-crystalline material is a model of typical glass–ceramic enamel. The analysis of the kinetic measurements demonstrated the non-steady state character of the investigated process of nucleation. Furthermore it is shown that the presence of small amounts of a surface tension lowering oxide (MoO_3) in the melt considerably decreases the interface energy at the crystal/melt boundary. This explains the role of MoO_3 and similar surface active oxides in inducing the bulk crystallization in glass–ceramic enamels.

1. Introduction

It is well known that by its very physical nature the nucleation process has a non-steady state character [1, 2]. The problem of the transient course of nucleation was raised for the first time by Zeldovich [3] and Frenkel [4]. The kinetics of non-steady state (or transient) nucleation is determined by the value of the non-steady state time lag, τ, which is proportional to the viscosity, η, in the case of crystallization of an undercooled melt (see [1]). Taking into account the high values of η typical for glass-forming melts, it is clear that non-steady state effects are of utmost importance in the crystallization kinetics of such systems. The expected τ values in the vicinity of the glass transition temperature, T_g, are of the order of hours.

Transient effects in the crystallization of glass-forming melts have been demonstrated for the first time in the case of a simple water soluble model glass ($(NaPO_3)_x$, see [1, 5, 6]). Later the non-steady state character of nucleation was proved also in the crystallization of more complex, three-component model silicate systems (e.g. Na_2O–BaO–SiO_2 glasses [7] and Na_2O–CaO–SiO_2 glasses [8] as well as in simple Li_2O–SiO_2 glasses [9, 10]. Certain isolated experimental data [11, 12] indicate that non-steady state effects can be observed in the crystallization of some glasses of the systems MgO–CaO–Al_2O_3–SiO_2(+ Fe_2O_3) and MgO–Al_2O_3–SiO_2(+ TiO_2). Such effects were found also in the kinetics of formation of a glass–ceramic material [13]. It is essental to note that the process of liquid phase separation, which is considered to some extent in the present investigation, may proceed also under non-steady state conditions [1, 2, 14]. In fact the transient character of the binodal liquid–phase segregation process was proved experimentally [15, 16] even before the establishment of the non-steady state character of crystallization in glass-forming systems.

The present paper provides further evidence on the applicability and necessity of the non-steady state approach in the quantitative treatment of phase formation in glass-forming melts and especially in technically important glass-forming systems. Some preliminary data in this respect have been reported in the already mentioned investigation [13]. The results obtained there stimulated the present study of the nucleation kinetics in a model lithium silicate melt of the system SiO_2–Al_2O_3–Li_2O–K_2O–MoO_3. By their composition and properties this melt and the partially crystalline material formed therefrom correspond to a typical glass–ceramic enamel.

Technical glass–ceramic enamels are silicate coatings with a relatively high content (over

0022–2461/84 $03.00 + .12

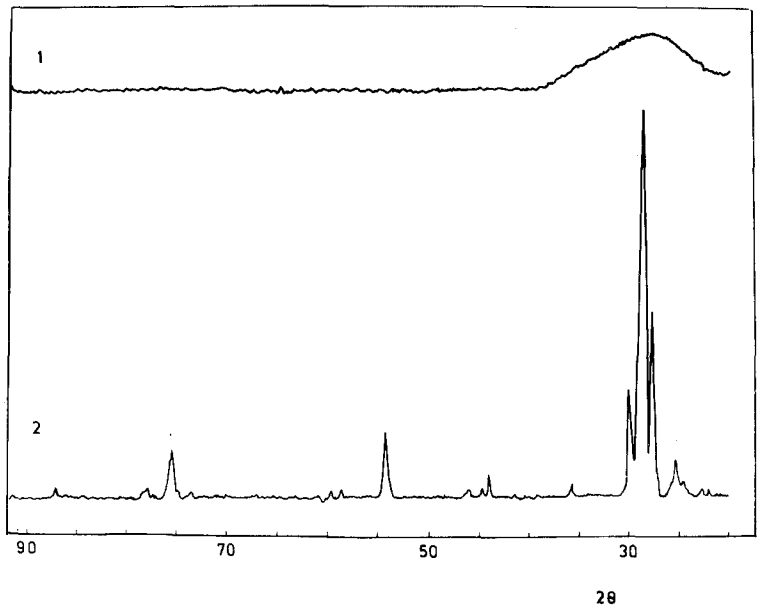

Figure 1 X-ray diffraction pattern of the initial model glass (curve 1) and of a glass sample after heat treatment (180 min at 850° C – curve 2).

30 wt %) of a finely dispersed and uniformly distributed crystalline phase obtained by an appropriate heat treatment. Such enamels are of considerable interest in silicate technology since they have better thermal resistance and higher mechanical strength when compared with usual glass–enamel coatings [17]. Bulk crystallization in technical glass–ceramic enamels is induced by the introduction of some oxides (such as TiO_2, CeO_2, P_2O_5, WO_3, Cr_2O_3, MoO_3, etc.) some of which (especially TiO_2 and probably CeO_2) may enhance liquid-phase separation, or could form upon cooling insoluble particles by precipitation from the melt, which acts as a crystallization core. However, the role of MoO_3 as a nucleation catalyst is of another type, as shown in the present study; this oxide does not form insoluble particles in the melt (at least at low concentrations), but it is a typical representative of surface tension lowering substances in silicate melts. This effect, as discussed in detail below, may change considerably the crystallization rate.

The high crystallite density normally achieved in the crystallization of such enamels as well as in typical glass–ceramic materials hampers the quantitative study of the crystallization process. In order to overcome this difficulty the nucleation kinetics are examined in the present work in thin films ($\sim 0.6\,\mu m$) blown from the initial glass as described in [13].

The complex nature of our model system required not only purely kinetic measurements of the crystallization process itself but also a number of additional investigations (X-ray diffraction, differential thermal analysis (DTA), electron microscopy, etc.) in order to elucidate the character, structure and composition of the phases formed upon heat treatment of the initial glass.

2. Experimental details

The main investigations were performed in a model melt having the composition 71.80 SiO_2, 1.63 Al_2O_3, 23.20 Li_2O, 2.20 K_2O, 1.17 MoO_3 (all mol %). This composition was found to be most suitable since only a single crystalline phase – the rhombic $Li_2O \cdot 2SiO_2$ is formed in the whole temperature range under investigation (540 to 620° C) as proved by X-ray diffraction, Fig. 1. Furthermore the main properties of this crystalline phase are well known from the literature.

The initial glass was melted at 1400° C in a platinum crucible; the melt was cast in steel moulds to give 12 mm × 12 mm × 80 mm samples which were quenched to room temperature. These samples were transparent and amorphous, as seen from the X-ray diffraction patterns (see Fig. 1).

The coefficient of thermal expansion, α, of the initial glass was $\alpha = 97 \times 10^{-7} °C^{-1}$ (Fig. 2b); completely crystallized samples have an α value of $106 \times 10^{-7} °C^{-1}$ corresponding to the value of $110 \times 10^{-7} °C^{-1}$ given in [18] for pure rhombic $Li_2O \cdot 2SiO_2$. The glass transition temperature, T_g, and the softening point, T_f, of our model glass were determined from the thermal expansion

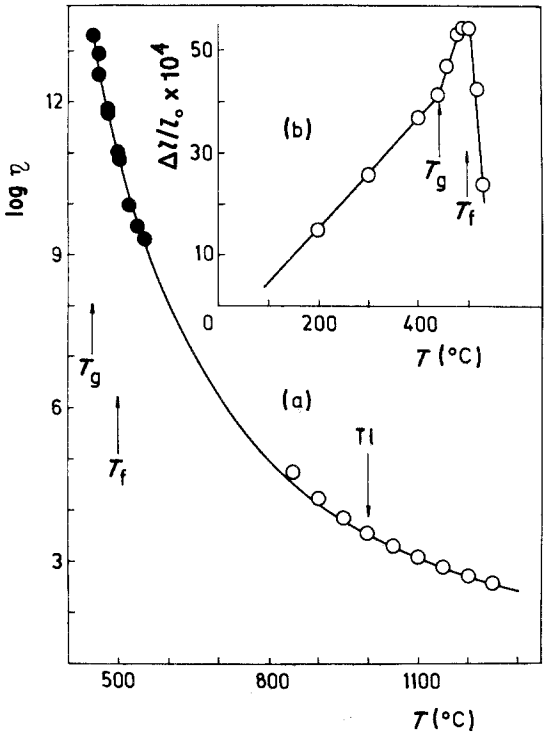

Figure 2 Temperature dependence of the viscosity, η, (curve a) and dilatometric curve (b) of the investigated glass-forming melt. The point T_l denotes the liquidus temperature of the crystalline phase in the system, according to DTA results.

curve (see Fig. 2b) as 450 and 508° C, respectively; after crystallization, the T_f of the samples increased up to 920° C.

Fig. 2b also shows results of the viscosity measurements performed. (1) A penetrometric device was used for $\log\eta$ from 9 to 13, and (2) a viscometer with a sinking platinum sphere for $\log\eta$ ranging from 2 to 5. The $\log\eta - T$ data given in Fig. 2a can be fitted with the Vogel–Fulcher–Tamman (VFT) equation

$$\log\eta = A_0 + \frac{B}{T - T_0} \qquad (1)$$

where $A_0 = -1.58$, $B = 3.99 \times 10^3$ and $T_0 = 460$ K. A comparison with the viscosity data of the pure $Li_2O \cdot 2SiO_2$ melt shows (cf. [19] where the VFT constants of pure $Li_2O \cdot 2SiO_2$ are given as $A_0 = -1.44$, $B = 3.37 \times 10^3$ and $T_0 = 460$ K) that the $\log\eta$ values of our model melt are about two orders of magnitude higher than those of the pure melt at equal temperatures. From Fig. 2a it can be seen that the viscometry values of T_g and T_f determined at $\log\eta = 13$ and $\log\eta = 11$ are in good agreement with the respective dilatometric determinations. Here and in Fig. 2 viscosity is given in poise ($= 10\,\mathrm{N\,sec\,m^{-2}}$).

Crystallization was investigated in the thin films as well as in the compact glass pieces; both types of samples were heat treated by being placed in the orifices of a small platinum bridge maintained at the desired temperature in an electric tube furnace. The temperature was measured by a thermocouple attached to the bridge. The time of the thermal treatment varied from 5 to 500 min and the temperature of the samples was maintained in the range 500 to 900° C to within an accuracy of ± 1° C. After quenching to room temperature, samples (glassy films and thin slices prepared from the compact pieces) were examined in polarized transmitted light in a NU-Zeiss microscope.

DTA records were obtained with Derivatograf MOM equipment in the temperature range 25 to 1500° C (heating rate of $7.5^\circ\,\mathrm{C\,min^{-1}}$ with α-Al_2O_3 standards) and the crystalline phases were identified using a Philips X-ray diffractometer (Cu$K\alpha$ radiation).

The microstructure of the massive samples was examined by transmission or scanning electron microscopy (SEM) (JEOL-100B instrument fitted with a SEM attachment). Platinum–carbon replicas as well as samples covered with gold (for SEM examinations) were used. Prior to replication or gold-shadowing the samples were treated with a dilute solution of hydrofluoric acid.

3. Results of structural and morphological studies

Fig. 3 illustrates the DTA curves of our model as well as those of a pure $Li_2O \cdot 2SiO_2$ glass. The curves are reconstructed from the original DTA records after graphical correction for the temperature difference sample-standard.

The X-ray diffractometry indicates that relatively pure $Li_2O \cdot 2SiO_2$ is formed from our melt since no deviation from the diffraction pattern of the pure crystalline substance could be observed (Fig. 1, curve 2).

Comparison of X-ray diffraction data with DTA shows that the single exothermic peak (at 655° C) on the DTA record (Fig. 3a) is caused by crystallization of $Li_2O \cdot 2SiO_2$ while the endothermic peak (at 1000° C) gives the liquidus temperature, T_l, in our melt. Fig. 3 also shows the DTA record for pure $Li_2O \cdot 2SiO_2$-glass; the endothermic peak at 1040 ± 10° C corresponds to the melting point

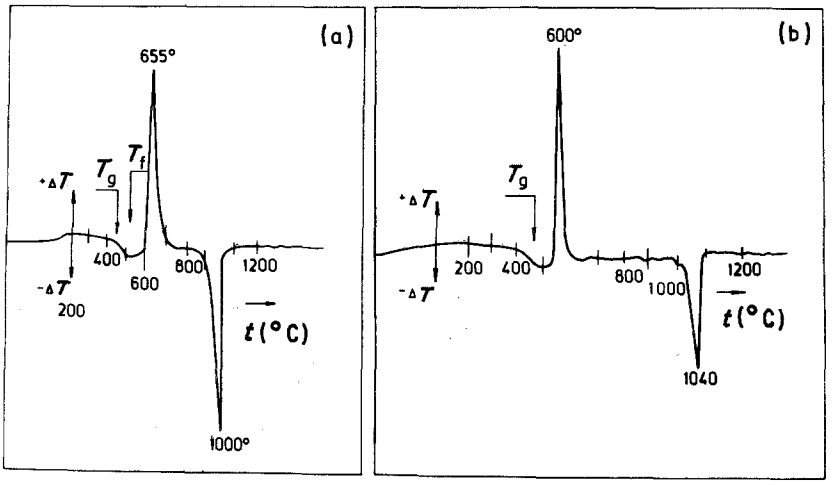

Figure 3 DTA curves of the composition investigated (a), and of the $Li_2O \cdot 2SiO_2$ melt (b): T_g and T_f obtained from viscosity measurements.

T_m of $Li_2O \cdot 2SiO_2$ given in [20]. A good coincidence is also seen for the T_g value of our glass determined by DTA (Fig. 3a) and the respective dilatometric and viscometric determinations of the same temperature according to Fig. 2.

Graphic integration showed that the area S under the endothermic peak (at 1000° C for our model composition, Fig. 3a) is equal to $1.2S_0$ where S_0 is the respective area under the melting peak of pure $Li_2O \cdot 2SiO_2$ (Fig. 3b). This indicates that the molar dissolution enthalpy, Δh_1, connected with the phase transition melt/crystal, is equal to $1.2\lambda_m$, the latter quantity being the enthalpy of melting of pure $Li_2O \cdot 2SiO_2$ (according to [20] $\lambda_{m_{Li_2O \cdot 2SiO_2}} = 12.9\,\text{kcal mol}^{-1}$). (1 cal = 4.18 J.)

Optical and electron microscopy indicated (Figs. 4 and 5) that in the material under investigation the crystallizing $Li_2O \cdot 2SiO_2$ forms characteristic spherulitic structures [9, 21]. The excellent mechanical properties of the lithium disilicate-type glass–ceramic coatings reported in the literature are possibly due to the mutual interpenetration of the structural elements (Fig. 6).

Electron microscopic examinations of our model composition gave no evidence for liquid-phase separation prior to or during the crystallization process.

4. Some basic theoretical considerations

The thermodynamic driving force of the crystallization process is given by the difference, $\Delta\mu$, in the chemical potentials of the melt and the respective crystal. In our case $Li_2O \cdot 2SiO_2$ crystallizes from a complex system – a SiO_2-rich multicomponent melt. If we consider this melt as a complex solvent phase, α, from which the pure crystalline phase β (in our case $Li_2O \cdot 2SiO_2$) is formed, $\Delta\mu$ can be expressed as

$$\Delta\mu \cong \int_{T_l}^{T} (S_\alpha^{(T)} - S_\beta^{(T)})\, dT \qquad (2a)$$

Here T_l is the liquidus temperature (according to Fig. 3a $T_l = 1273\,\text{K}$) and $S_\alpha^{(T)}$ and $S_\beta^{(T)}$ are the molar entropies of the molten matrix phase and the crystal at temperature T. The integral in Equation 2a can be calculated if the entropy difference $(S_\alpha - S_\beta) \equiv \Delta S^{(T)}$ is known. Expanding, as usual, $\Delta\mu$ in a Taylor series, at the liquidus temperature T_l, we obtain

$$\Delta\mu \cong \Delta S_l \left[1 - \frac{\Delta C_p(T_l)}{2\Delta S_l} + \frac{\Delta C_p(T_l)}{2\Delta S_l}\frac{T}{T_l}\right]\Delta T \qquad (2b)$$

Here $\Delta S_l = \Delta h_l / T_l$ is the entropy of dissolution at $T = T_l$, Δh_l is the already stated enthalpy of dissolution of $Li_2O \cdot 2SiO_2$, $\Delta T = T_l - T$ is the undercooling, and $\Delta C_{p(T_l)}$ denotes the difference in the molar heat capacities of the matrix melt and the crystal at T_l. It is known that for typical glass-forming systems $\Delta C_p(T_m)/\Delta S_m \approx 2$ [22], where $\Delta S_m = \lambda_m / T_m$ is the molar entropy of melting. If we assume that in our case $\Delta C_p(T_l)/\Delta S_l \approx 2$, Equation 2b gives

$$\Delta\mu \cong \Delta S_l \Delta T \frac{T}{T_l} = \frac{\Delta h_l}{T_l}\Delta T \frac{T}{T_l} \qquad (2c)$$

Such an assumption is supported by the stated DTA data, according to which $\Delta h_l = 1.2\lambda_m$, i.e.

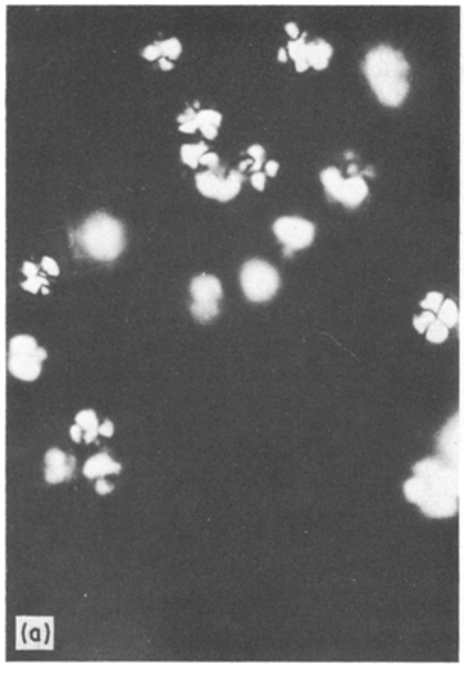

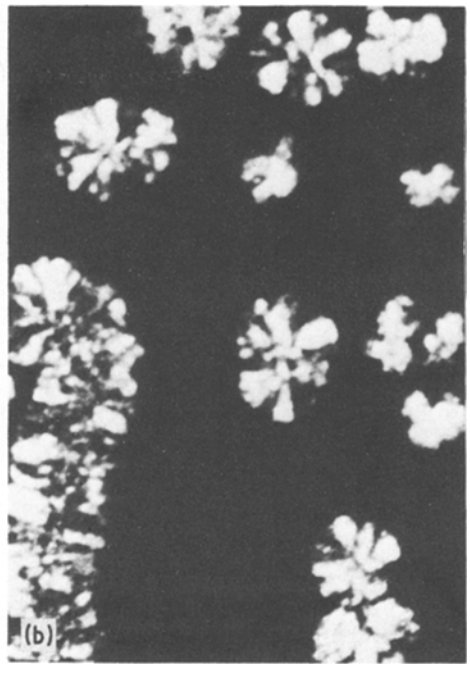

Figure 4 Micrographs of $Li_2O \cdot 2SiO_2$ spherulites formed in massive samples heat treated at (a) 564° C for 120 min, (b) 564° C for 420 min (c) 650° C for 90 min. Crossed nicols: (a) × 160, (b) × 25 and (c) × 63.

the enthalpy of mixing, Δh_{mix}, amounts in our case to only $0.2\lambda_m$. So it can be expected that the differences ΔS_l and $\Delta C_{p(T_l)}$ are close to the respective values for the pure substance (ΔS_m, $\Delta C_{p(T_m)}$). In accordance with the DTA finding and the stated values of λ_m, Δh_l in the further analysis is assumed to be 15.8 kcal mol^{-1}.

It is well known that two model approaches are possible in the theory of phase formation – the atomistic treatment and the classical model of nucleation. The limits of validity of these two models depend on the number, n_k, of building units in the nucleus; as a rule at $n_k < 5$ to 10 the atomistic model is preferable. Thus a preliminary estimate of n_k is necessary.

In the framework of the classical (or capillary) model of phase formation the radius r_k of the nucleus is determined by the Thomson–Gibbs equation

$$r_k = \frac{2\sigma V_m}{\Delta\mu} \tag{3}$$

In our case σ is the interfacial energy at the melt/crystal boundary and V_m denotes the molar volume of the newly formed crystal. The value of σ can be estimated, e.g. by means of the Scapski–Turnbull formula [23]

$$\sigma = \gamma_0 \frac{\Delta h_l}{N_a^{1/3} V_m^{2/3}} \tag{4}$$

Here N_A denotes the Avogadro number and γ_0 is a numerical coefficient which in the case of crystallization from solutions has an approximate

Figure 5 $Li_2O \cdot 2SiO_2$ spherulites formed in a thin film sample heat treated at 650° C 5 min. Crossed nicols, × 160.

value of 0.2 [24]. Introducing into Equation 4 the stated value of Δh_1 and taking $V_m = 61.1\ cm^3\ mol^{-1}$ [20], $\sigma = 1.01 \times 10^{-5}\ J\ cm^{-2}$ is obtained. The simplest assumption of a spherical equilibrium form of the nucleus (cf. Equations 2c, 3 and 4) gives

$$n_k = \tfrac{4}{3}\pi(2\gamma_0)^3\left(\frac{T_1^2}{T\Delta T}\right)^3 \qquad (5)$$

and leads to a value of $n_k \approx 22$ to 30 under our conditions. This preliminary assessment shows that the classical nucleation theory can be applied at least qualitatively in the analysis of the following experimental results on the kinetics of nucleation.

According to this theory (cf. [1] and references therein) the temperature dependence of the steady state rate of nucleation I_0 in an undercooled melt having viscosity η can be described with sufficient accuracy as

$$I_0 \cong A\frac{1}{\eta}\exp\left(-\frac{W_k}{kT}\right) \qquad (6)$$

where

$$W_k = \frac{16}{3}\frac{\pi\sigma^3 V_m^2}{(\Delta\mu)^2} \qquad (7)$$

is the work of nucleation as defined within the framework of the classical approach, k is the Bolzmann constant and

$$A = \frac{N_A}{V_m}4\pi r_k^2\frac{kTZ'}{d_0^5}\frac{1}{n_k}\left(\frac{W_k}{3\pi kT}\right)^{1/2} \qquad (8)$$

In Equation 8 d_0 is the mean interatomic distance in the melt and Z' takes into account the difficulties connected with the incorporation of the molecules of the initial phase in the critical nucleus of the new phase. In the case of heterogeneous nucleation

$$W_k^* = W_k\phi \qquad (9)$$

where $0 \leqslant \phi \leqslant 1$ is the activity of the substrate with respect to the nucleation process.

From Equations 2c, 6, 7 and 9 it follows that

$$I_0^* \cong A\frac{1}{\eta}\exp\left(-\frac{K_3}{T^3\Delta T^2}\right) \qquad (10)$$

where

$$K_3 = \frac{16}{3}\pi\frac{\sigma^3\phi V_m^2 T_1^4}{(\Delta h_1)^2}\frac{1}{k} \qquad (11)$$

Taking into account Equations 6 (with $W_k \equiv$

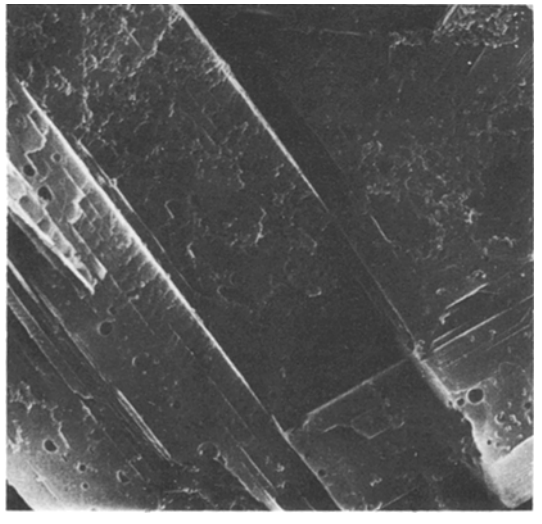

Figure 6 Characteristic layer structure of $Li_2O \cdot 2SiO_2$ for fully crystallized sample heat treated for 300 min at 700° C. SEM of a freshly fractured sample, leached for 15 sec with 2% hydrofluoric acid.

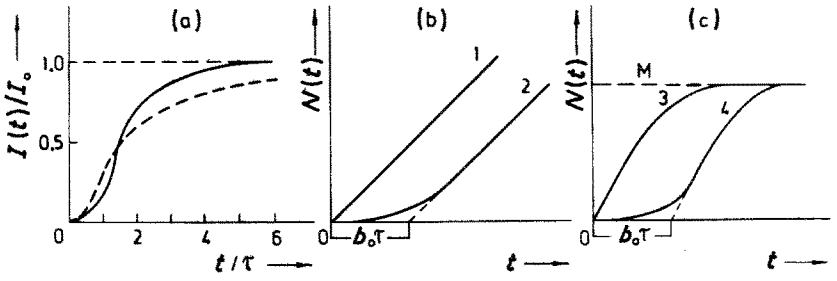

Figure 7 Kinetics of transient homogeneous nucleation (a) and theoretical $N_{(t)}$–t curves (b) and (c). (a) $I_{(t)}$ curves: full line, according to the more accurate solution (Equation 16). Broken line, the approximate solution (Equation 14) given by Zeldovich. (b) Homogeneous nucleation (initial stage): curve 1, steady state process; curve 2, non-steady state nucleation. (c) Heterogeneous nucleation: curve 3, steady state case; curve 4, non-steady state case.

W_k^*) and 10 it follows that

$$W_k^* = \frac{K_3 k}{T^2 \Delta T^2} \tag{12}$$

At sufficiently small temperature intervals the temperature dependence of the viscosity, η, determined by the VFT Equation 1 may be represented by an exponential expression given by

$$\eta = A' \exp\left(\frac{U_\eta}{kT}\right) \tag{13}$$

where U_η denotes the activation energy of viscous flow in the temperature range under consideration and A' is a constant.

The time dependence of the rate of nucleation under non-steady state conditions can be written approximately as [1–3]

$$I_{(t)} = I_0 \exp\left(-\frac{\tau}{t}\right) \tag{14}$$

where

$$\tau = -\frac{b_0 kT}{\left[\frac{\partial^2 W}{\partial n^2}\right]_{n=k} D_k} \tag{15a}$$

is the transient time lag, $b_0 \approx 1$ and D_k is the flux of molecules from the ambient phase to the critical cluster [25].

Following the argument given in [1, 2], τ can be written in the case of crystallization of an undercooled melt as

$$\tau = \sigma \left(\frac{N_A}{\Delta\mu}\right)^2 (d_0)^5 \eta \frac{1}{Z'} \tag{15b}$$

In the case of formation of isotropic phases (e.g. in the case of liquid phase separation) the coefficient $Z' \approx 1$ [14, 26], whereas upon formation of crystalline phases $Z' \approx 10^{-3}$ to 10^{-6} [2, 26]. From Equation 15b it follows [1, 2] that measurable non-steady state effects ($\tau > 10^2$ sec) should be expected when viscosities of the order of 10^6 to 10^9 poise are reached, i.e. under conditions at which most crystallization processes in technical glass-forming systems take place.

A more accurate solution of the non-steady state problem determines $I_{(t)}$ as [25]

$$I_{(t)} = I_0 \left[1 + 2 \sum_{m=1}^{\infty} (-1)^m \exp\left(-m^2 \frac{t}{\tau}\right)\right] \tag{16}$$

Equations 14 and 16 are illustrated in Fig. 7a.

Multiplication of Equations 10 and 15b gives

$$I_0^* \tau = C \exp\left(-\frac{K_3}{T^3 \Delta T^2}\right) \tag{17}$$

where $C = A\sigma(N_A/\Delta\mu)^2 (d_0)^5 (1/Z')$ is practically a constant with respect to the exponential dependence. It is of particular significance that according to Equation 17 the product $I_0^* \tau$ does not depend on the viscosity, η, so that its temperature course is determined only by the exponent $k_3/T^3\Delta T^2$.

As shown in [1, 2], in order to elucidate the steady state character of the nucleation kinetics, it is necessary to analyse the character of the $N_{(t)} - t$ curves, i.e. the time dependence of the number N of nuclei grown at the moment t. When transient effects are negligible, the stationary rate of nucleation is instantaneously established. In this case it follows from

$$N(t) = \int_0^t I(t)\, \mathrm{d}t \tag{18}$$

with $I_{(t)} = \text{constant} = I_0$ that

$$N(t) = I_0 t \tag{19}$$

Using Equation 18 and the approximate solution 14, the following expression can be derived* [2]:

$$N(t) = I_0 t\left[\exp\left(-\frac{\tau}{t}\right) + \frac{\tau}{t}E_i\left(-\frac{\tau}{t}\right)\right] \quad (20)$$

which is illustrated in Fig. 7b.

Strictly speaking, Equations 19 and 20 refer only to homogeneous nucleation. In the case of heterogeneous nucleation, when M highly active crystallization sites are present per unit volume of the melt (e.g. insoluble crystallization cores), nucleation will proceed practically only at these sites. In such a case even under steady state conditions the heterogeneous nucleation rate I_0^* will be time dependent due to the depletion of the initial active sites. According to [2], here

$$N(t) = M[1 - \exp(-I_0^* t)] \quad (21a)$$

For heterogeneous non-steady state nucleation on M active sites (as shown in [2]):

$$N(t) = M\left(1 - \exp\left\{-I_0^* t\left[\exp\left(-\frac{\tau}{t}\right) + \frac{\tau}{t}E_i\left(-\frac{\tau}{t}\right)\right]\right\}\right) \quad (21b)$$

Both dependences are illustrated in Fig. 7c. It is seen once again that the curve for the transient case is shifted by $b_0\tau$ with respect to the origin (Equation 21a). As in the homogeneous case, this shift is the fundamental experimental criterion for determining the character of the nucleation process. The maximum number, N_S, of crystallites in the saturated region of the $N_{(t)}$–t curves will be equal to M [2, 26].

Saturated regions in the $N_{(t)}$–t curves are to be expected in principle also in the case of homogeneous nucleation since each process of phase formation is accompanied by a depletion of the space available for nucleation. Strictly speaking, the curves in Fig. 7b should be considered only as an approximate description of the initial stages of nucleation. In the homogeneous case the maximum number N_s of crystallites formed in the melt under given conditions is generally a function of the ratio I/V, where V is the growth rate of the individual crystallites [27].

A thorough study of the role of active centres in nucleation performed in [28] indicates that at moderate I/V values (i.e. for small I_0^* values or large V values) N_s is not directly determined by M, as in Equation 21, but will be a function of I and V (as in the homogeneous case):

$$N_s = \text{constant}\,\frac{(I_0^*)^{3/5}}{V^{6/5}} \quad (22)$$

The atomistic approach gives for the rate of nucleation an equation of the type $I = (1/\eta)\exp(W_k)$ but the specific character of this model defines W_k in a different way without use of a macroscopic value of the surface energy σ. Kashchiev [29] has shown that irrespective of the concrete model of nucleation – atomistic or capillary – the number of building units in the nucleus can be determined in the case of crystallization from a melt as

$$n_k = 2.3kT\frac{d\log I_0^*}{d\Delta\mu} - \frac{U_\eta}{kT}\frac{dkT}{d\Delta\mu} \quad (23a)$$

Using Equation 2c for $\Delta\mu$ it follows:

$$n_k = 2.3kT\frac{d\log I_0^*}{d\Delta\mu} - \frac{U_\eta}{kT}\frac{kT_1}{\Delta S_1(T_1 - 2T)} \quad (23b)$$

Here again Equation 1 was used for η, so $d\log I_0^*/d\Delta\mu$ can be calculated from the $\log I_0^*$ against $\Delta\mu$ plot of experimental data of nucleation and U_η from the $\log\eta$ against $1/T$ dependence in the same temperature range.

5. Experimental data and discussion of nucleation kinetics

Fig. 8 summarizes the results of a series of measurements giving the number N of grown $Li_2O \cdot 2SiO_2$ crystallites determined in thin films as a function of the time t of isothermal heat treatment. The different temperatures are indicated as a parameter at each $N_{(t)}$–t curve. The course of these $N_{(t)}$–t curves follows qualitatively the dependence given by Equation 21b (see also Fig. 7c) and is similar to the previously observed [13] $N_{(t)}$ functions. An induction period is clearly seen, followed by a linear increase of the number of crystallites N and subsequent saturated region. It is seen that the number of crystallites in the region of saturation increases from $16 \times 10^6\,cm^{-2}$ (corresponding to $26 \times 10^{10}\,cm^{-3}$) at 542°C to $26 \times 10^6\,cm^{-2}$ (or $43 \times 10^{10}\,cm^{-3}$) at 618°C.

The rates of nucleation $I_{0i}^* = dN_i/dt$ corresponding to the linear part of the $N_{(t)}$–t curves are given in Fig. 9 in coordinates $\log I_0^*$ against $\Delta\mu$ according to Equation 23b. The value of n_k obtained in this

*Here E_i denotes the integral exponential function.

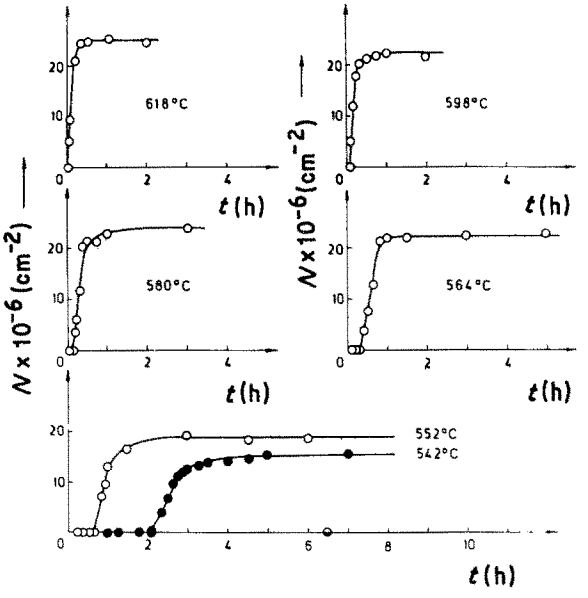

Figure 8 Experimental $N_{(t)}$–t curves for the crystallization of $Li_2O \cdot 2SiO_2$ for different temperatures (given for each curve in °C).

way ($n_k = 20$ to 30) is in agreement with the previous semitheoretical estimation (see Equation 4) and shows again that the classical model of the nucleation theory may be applied.

For this reason in Fig. 10 (curve 2) our experimental data for I_0^* and η are given as a $\log I_0^* \eta$ against $1/T^3\Delta T^2$ plot (cf. Equations 10 and 13). As it should be expected, a straight line with a slope $K_3 = 2.7 \times 10^{15}(K^5)$ is observed. Substituting this value into Equation 12, in order to determine W_k^* and using the relation $n_k = 2W_k^*/\Delta\mu$ [29] for the number of the building units, $n_k = 20$ to 30 is obtained once again.

Using the value of σ estimated by Equation 4 (i.e. $\sigma = 1.01 \times 10^{-5}\,J\,cm^{-2}$) in order to calculate W_k (see Equation 7) and W_k^* (from Equation 12), $\phi = 0.98$ to 1 is obtained (see Equation 9). Consequently, $\sigma = 9.8$ to $10.0 \times 10^{-6}\,J\,cm^{-2}$ can be determined from Equation 11. This result is an indication that our process may be treated practically as a case of homogeneous nucleation.

From Fig. 10 (curve 2) A is determined to be $2 \times 10^{29}\,cm^{-3}\,sec^{-1}$. This value of A is about 5 orders of magnitude lower than that expected

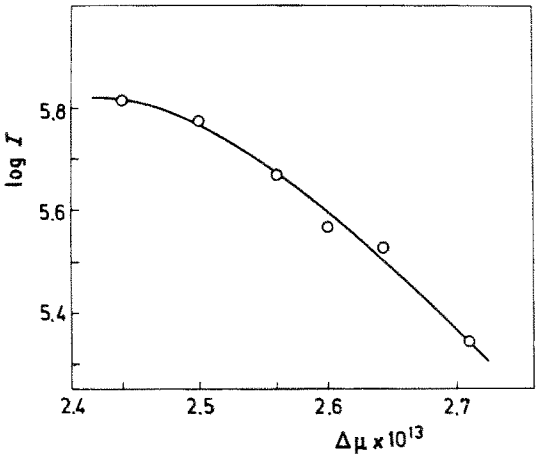

Figure 9 Log I_0^* against $\Delta\mu$ plot for determination of the number n_k of building units in the nucleus.

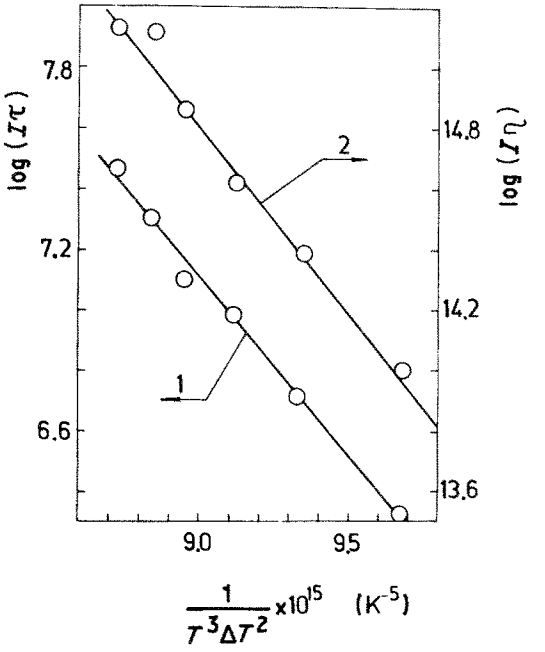

Figure 10 Log $I\tau$ and log $I\eta$ against $1/T^3\Delta T^2$ (curves 1 and 2) plots according to Equations 10, 13 and 17.

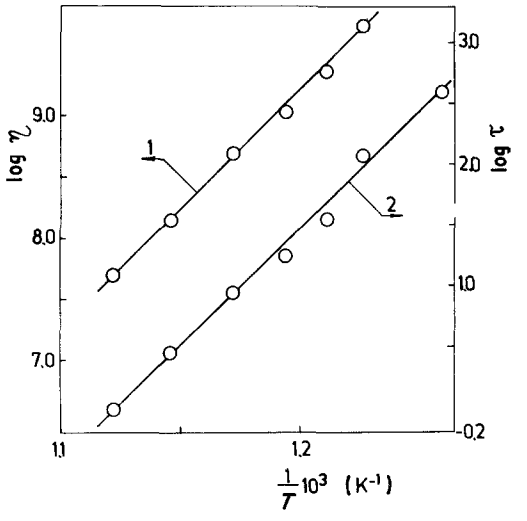

Figure 11 The temperature dependence of η as $\log\eta$ against $1/T$ (curve 1) and of the induction period of nucleation, τ, as $\log\tau$ against $1/T$ (curve 2).

from Equation 8. (The theoretical value of A with $Z' = 4 \times 10^{-4}$, $d_0 = 4.7 \times 10^{-8}$ and the stated value of W_k is $A = 5.4 \times 10^{34}$). However, taking into account that at present the nucleation theory determines I_0 only with an exponential accuracy, such a difference in the calculated and actual pre-exponential constants is quite satisfactory. In fact d_0 which participates in Equation 8 in the power of eight can be only estimated from a more or less arbitrary chosen effective value for the molecular weight of our melt.

In Fig. 11 the experimental data for the temperature dependence of the viscosity, η, according to Fig. 1 and Equation 1 are plotted in coordinates $\log\eta$ against $1/T$ (Equation 13) for the sufficiently narrow temperature range under investigation. The induction periods from Fig. 8 are also given in Fig. 11 according to Equations 13 and 15b in the form of $\log\tau$ against $1/T$. It is seen that as expected in the stated temperature range $\log\eta$ and $\log\tau$ are linear with respect to $1/T$. Moreover one and the same value of the activation energy $u_\eta \approx U_\tau \approx 90\,\mathrm{kcal\,mol^{-1}}$ is obtained.

It follows from Equation 17 that plotted as $\log I_0^* \tau$ against $1/T^3\Delta T^2$ a straight line should also be expected (Fig. 10, curve 1). This plot gives a direct proof of the transient character of the induction period observed in Fig. 8.

Fig. 12 gives further support of the non-steady state character of nucleation; here our experimental data (for the ascendant part of the $N_{(t)}$–t curves in Fig. 8) are plotted as $N(t)/I_0\tau$ against t/τ [25] according to Equation 16. Obviously, this equation yields a satisfactory description of the nucleation kinetics in our model melt.

Fig. 13 summarizes the temperature dependence of the non-steady state time lag, τ, and the rate of nucleation for the whole temperature range under investigation. The $\log I_0$ and $\log\tau$ against T curves are plotted according to Equations 10 and 15b with the experimentally determined values of η, A and K_3. The theoretical $\log\tau$ against T dependence describes the experimentally determined temperature dependence of $\log\tau$ when $Z' = 4 \times 10^{-4}$ is introduced into Equation 15b.

6. Discussion

The present investigation leads to the following

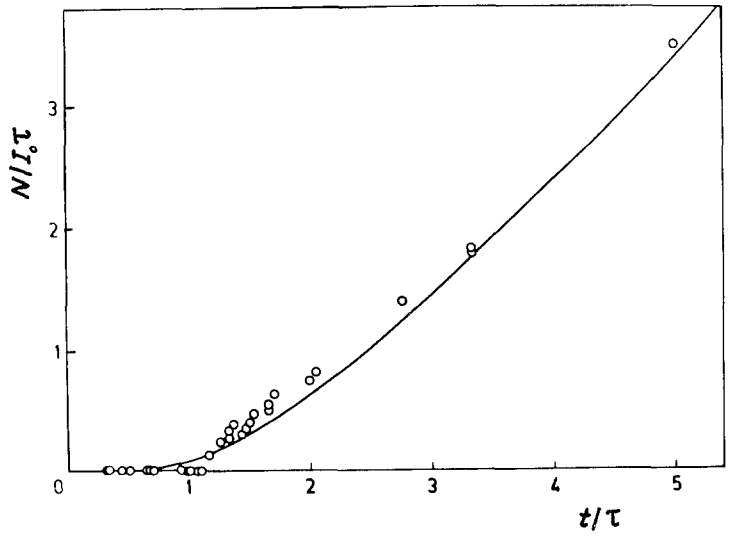

Figure 12 Comparison of experimental data with theory of non-steady state kinetics of nucleation. Full line: $N_{(t)}$–graph according to Equations 16 and 18 [25].

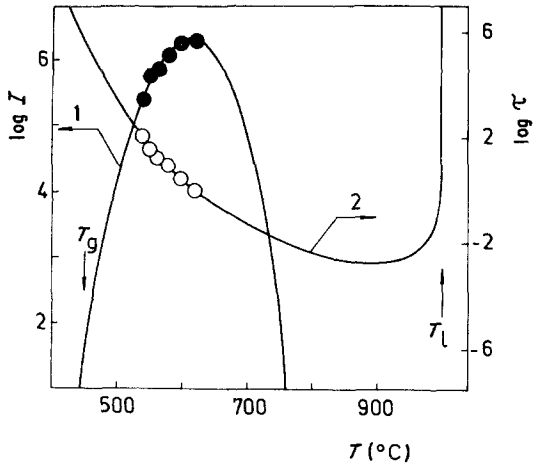

Figure 13 Temperature dependence of $\log I_0$ and $\log \tau$ over the whole investigated temperature interval. Curve 1 – $\log I$ against T (in °C); black points experimental I_0-data (in number of nuclei $cm^{-2}\,min^{-1}$. Curve 2 – $\log \tau$ in min against t (in °C); white points experimentally determined induction periods. T_l and T_g are the liquidus and vitrification temperatures respectively.

more or less general conclusions concerning the kinetics of nucleation in our glass–ceramic enamel.

According to the arguments given in Section 5, the induction periods observed in the $N_{(t)}$–t curves can be treated as non-steady state time lags. This is especially clearly seen in Fig. 12. The $N(t)/I_0\tau$ against t/τ plot has proved already the non-steady state crystallization kinetics of $Li_2O \cdot 2SiO_2$ from its own melt (cf. [9]). It seems that the $\log I_0\tau$ against $1/T^3\Delta T^2$ plot has been used here for the first time as a verification of the non-steady state character of the crystallization process in the case of crystallization from an undercooled melt. Convincing evidence in this respect is given also by the $\log \eta$ against $1/T$ and $\log \tau$ against $1/T$ juxtaposition. Values of Z' similar to those found in the present investigation ($Z' \approx 10^{-4}$) were also observed in the foregoing study of the transient nucleation kinetics of $NaPO_3$ model glass [2, 5] as well as in the crystallization kinetics of an enstatite type glass–ceramic material [13].

No artificial nucleation agents in the form of insoluble substrates, the so-called crystallization cores were introduced into our model melt but nevertheless an overall bulk crystallization with a relatively high nucleus density was observed. Electron microscopic examinations gave no evidence for the existence of any inhomogeneities in our glass which could be interpreted as crystallization cores formed prior to crystallization and, as stated above, no crystalline phase other than $Li_2O \cdot 2SiO_2$ could be determined by X-ray diffraction or DTA. Liquid phase separation prior to crystallization was also excluded to a great extent (cf. Section 2) and a value of ϕ ranging from 0.98 to 1 follows from the comparison of W_k^* with W_k. Thus nucleation is either homogeneous or heterogeneous on unidentified, accidental, very small and very inactive centres. The slight temperature dependence of the number N_s of crystallites in the saturated region of our $N_{(t)}$ curves can be satisfied by both situations (cf. Section 4 and [28]). Nevertheless (as stated above) in our model melt a uniform bulk crystallization process with a very high density of crystallites ($N_s \approx 10^{11}\,cm^{-3}$) is achieved and nucleation rates are observed which are approximately two orders of magnitude higher than those found in [19] for the pure $Li_2O \cdot 2SiO_2$ melt (if we compare the maximal value of I in both cases). This is still more surprising taking into account that the viscosity η of our model melt is about two orders of magnitude greater than the viscosity of the pure $Li_2O \cdot 2SiO_2$ melt (see Section 2). Thus the enhanced nucleation of our melt should be explained by a lowering of W_k due to a decrease of the interfacial energy σ (cf. Equation 7).

It is known that the surface energy at the crystal–melt interface σ may be connected with the value of surface energy at the vapour–melt interface σ_0 by Gorskii's rule [30]: $\sigma = \alpha\sigma_0$ where in the case of low melting organic melts it has been found that $\alpha \approx 0.1$. The value of σ_0 for pure $Li_2O \cdot 2SiO_2$ melt is approximately 3.2 to $3.3 \times 10^{-5}\,cm^{-2}$ [31]. As already stated, the addition of MoO_3 considerably decreases σ_0 of silicate melts [32, 33] (e.g. it is known that 2 mol% MoO_3 decreases σ_0 of Na_2O–SiO_2 melts from 2.8 to $2.0 \times 10^{-5}\,J\,cm^{-2}$ [33], i.e. by about 30%).

Rowlands and James [19] in their investigation of the nucleation of $Li_2O \cdot 2SiO_2$ from its own melt have found from the $\ln I_\eta$ against $1/T\Delta T^2$ plot $\sigma \approx 2 \times 10^{-5}\,J\,cm^{-2}$. A similar result ($\sigma \approx 1.8$ to $2 \times 10^{-5}\,J\,cm^{-2}$) has been obtained for $Li_2O \cdot 2SiO_2$ by Kalinina *et al.* [10]. This value considerably exceeds that obtained by us in the present study ($\sigma \approx 1 \times 10^{-5}\,J\,cm^{-2}$). In spite of the fact that both values of σ are not absolutely reliable, a decrease in σ is observed, corresponding to the tendency which can be expected accounting for Gorskii's rule. In our opinion this decrease in σ may explain the considerably higher nucleation

rates as well as the increase in the number of crystallites in our system.

This result elucidates the influence of some oxides similar to MoO_3 (e.g. WO_3, V_2O_5, Cr_2O_3, etc.) in inducing the bulk crystallization of glass–ceramic enamels. Our model melt indicates also considerable possibilities for the modification of nucleation kinetics by addition of small quantities of surface active substances such as MoO_3 in silicate melts. The effect of surface active additives in the kinetics of nucleation is well known and has been investigated in detail in [35] where the lowering of σ has been discussed in terms of Sziskowski's equation, well known from the physical chemistry of surface active organic substances and their action in aqueous solutions.

The results of the present investigation show that non-steady state effects may be of decisive importance in the interpretation of the crystallization phenomena in such technical glass-forming melts as glass–ceramic enamels, especially when the viscosity of the system is over 10^6 to 10^8 dPa.

Acknowledgements

We would like to thank Professor W. Vogel (Jena, DDR) and Professor O. Mazurin (Leningrad, USSR) for the viscosity measurements on our model melt performed in their laboratories. Thanks are also due to Dr D. Kashchiev (Sofia) for the helpful discussions concerning some of the main results of the present investigation.

References

1. I. GUTZOW, *Contemp. Phys.* **21** (1980) 121, 243.
2. I. GUTZOW and S. TOSCHEV, in "Advances in Nucleation and Crystallization in Glasses", edited by L. L. Hench and S. W. Freiman (American Ceramic Society, Columbus, Ohio, 1971) p. 10.
3. J. B. ZELDOVICH, *Acta Phys. Khim. URSS* **18** (1943) 1.
4. J. FRENKEL, "Kinetics Theory of Liquids" (Dover, New York, 1955) p. 398.
5. I. GUTZOW, S. TOSCHEV, M. MRINOV and E. POPOV, *Kristall u. Technik* **3** (1978) 37, 337, 485.
6. I. GUTZOW, E. POPOV, S. TOSCHEV and M. MARINOV, Proceedings of the Symposium on Crystal Growth, VII ICC, Moscow, July 1966, Rost Kristallov, Vol. 8, Part II (Izd. Nauka, Moscow, 1968) p. 95.
7. D. G. BURNETT and R. W. DOUGLAS, *Phys. Chem. Glasses* **12** (1971) 117.
8. Z. STRNAD and R. W. DOUGLAS, *ibid.* **14** (1973) 33.
9. P. F. JAMES, *ibid.* **15** (1974) 95.
10. A. M. KALININA, V. M. FOKIN and V. N. FILIPOVICH, *Fizika Khim. Stekla* **3** (1977) 122.
11. P. R. ROGERS, *Mineral. Mag.* **37** (1970) 741.
12. W. ZDANIEWSKI, *J. Amer. Ceram. Soc.* **61** (1978) 199.
13. I. GUTZOW, E. ZLATEVA, S. ALYAKOV and T. KOVATSCHEVA, *J. Mater. Sci.* **12** (1977) 1190.
14. I. GUTZOW, in "The Vitreous State" (Discussions of the Faraday Society, No. 50, London, 1971) p. 236.
15. J. J. HAMMEL, *J. Phys. Chem.* **46** (1967) 2234.
16. S. M. OHLBERG and J. J. HAMMEL, in Proceedings of the 7th International Congress on Glass, Brussels, 1965. 28VI–3VII, Number 32, p. 1.
17. A. A. APPEN, Temperaturoustoichivie Neorganicheskie Pokritiya" (Khimia, Leningrad, 1976) p. 116.
18. H. M. PAVLUSHKIN, "Osnovi Tekhnologia Sitalov" (Stroitelstvo, Moscow, 1970) p. 330.
19. E. G. ROWLANDS and P. F. JAMES, *Phys. Chem. Glasses* **20** (1979) 6, 1.
20. I. BARIN and O. KNACKE, "Thermochemical Properties of Inorganic Substances" (Springer, Berlin, 1973).
21. M. A. BEZBORODOV, "Samoproizvolnaya Kristalizacia Silikatnikh Stekol" (Nauka i Technika, Minsk, 1981) pp. 109, 209.
22. I. GUTZOW, in "The Physics of Non-Crystalline Solids", edited by G. H. Frischat (Trans. Technical Publications, Aedermannsdorf, 1977) p. 356.
23. D. TURNBULL and M. H. COHEN, in "Modern Aspects of the Vitreous State" edited by I. D. Mackenzie (Butterworths, London, 1960) p. 38.
24. V. KAHLWEIT, *Z. Phys. Chem. NF* **28** (1961) 245.
25. D. KASHCHIEV, *Surf. Sci.* **14** (1969) 209.
26. S. TOSCHEV and I. GUTZOW, *Kristall u. Technik* 7 (1972) 43.
27. M. VOLMER, "Kinetik d. Phasenbildung" (Ver. Th. Steinkopt, Dresden u. Leipzig, 1939) p. 206.
28. I. MARKOV and D. KASHCHIEV, *J. Cryst. Growth* **13/14** (1972) 131.
29. D. KASCHIEV, *J. Chem. Phys.* **76** (1982) 5098.
30. F. K. GORSKII, "Kristallizatsiya i fazovie perekhodi" (Izd. Akad. Nauk BSSR, Minsk, 1962) p. 58.
31. O. V. MAZURIN, M. V. STRELSINA and T. P. SHVAIKO-SHVAIKOVSKAIA, "Svoistva Stekla i Stekloobrazuiushchikh Rasplavov" Vol. I (Nauka, Leningrad, 1973) p. 178.
32. W. A. WEYL and E. C. MARBOE, "The Constitution of Glasses. A Dynamic Interpretation" Part I (John Wiley and Sons, New York, London, Sydney, 1964) p. 645.
33. A. A. APPEN, *Zh. Fiz. Khim.* **26** (1952) 1404.
34. I. I. KITAIGORODOSKI, "Tekhnologia Stekla" Stroitelstvo, Moscow, 1961) p. 37.
35. R. KAISCHEW and B. MUTAFCHIEV, *Izv. Khim. Inst.-BAN* 7 (1959) 145, 176.

Received 24 January
and accepted 18 May 1983